Advanced Concepts and Applications of Laser Pulses

Juan Landers

Advanced Concepts and Applications of Laser Pulses

Edited by **Juan Landers**

Clanrye International

New Jersey

Published by Clanrye International,
55 Van Reypen Street,
Jersey City, NJ 07306, USA
www.clanryeinternational.com

Advanced Concepts and Applications of Laser Pulses
Edited by Juan Landers

International Standard Book Number: 978-1-63240-014-7 (Hardback)

Printed in the United States of America.

Advanced Concepts and Applications of Laser Pulses

Preface

The purpose of the book is to provide a glimpse into the dynamics and to present opinions and studies of some of the scientists engaged in the development of new ideas in the field from very different standpoints. This book will prove useful to students and researchers owing to its high content quality.

This book, written by renowned experts from across the globe, aims to elucidate the diverse concepts of laser pulses. The book explains characteristics of laser pulse creation, classification and applications. It even illustrates accomplishments made in designs, experiments and theories. The book contains examples of laser procedures in biomedical areas, and tremendously high power systems used for substance processing and water decontamination. This book will help students, managers and engineers to understand laser technology better.

At the end, I would like to appreciate all the efforts made by the authors in completing their chapters professionally. I express my deepest gratitude to all of them for contributing to this book by sharing their valuable works. A special thanks to my family and friends for their constant support in this journey.

Editor

Contents

Section 1

Unusual Applications

Progress in High Average Power, Short Pulse Solid State Laser Technology for Compton X-Ray Sources

Akira Endo

Additional information is available at the end of the chapter

1. Introduction

Laser Compton X-ray source has been developing in more than decade as an accelerator-laser hybrid technology to realize a compact, high brightness short wavelength source. The basic principle is similar to an undulator emission, in which a high intensity laser field plays as the modulating electromagnetic field. Basic principle of the laser Compton X-ray source is explained in this chapter with recent examples of phase contrast imaging of bio samples. Single shot imaging is critical for many practical applications, and the required specification is explained as the laser pulse must exceeds some threshold parameters. It is already well studied on the optimization of the laser-Compton hard X-ray source by single shot base (John, 1998, Endo, 2001). Experimental results agreed well with theoretical predictions. Highest peak brightness is obtained in the case of counter propagation of laser pulse and electron beam bunch with minimum focusing area before nonlinear threshold (Babzien et.al, 2006: Kumita, et.al, 2008). The new short wavelength light source is well matured to demonstrate a single-shot phase contrast bio imaging in hard X-ray region (Oliva, et.al, 2010). The employed laser is a ps CO_2 laser of 3J pulse energy (Pogorelsky, et.al, 2006), but the laser system is not an easy and compact one for further broad applications in various laboratories and hospitals.

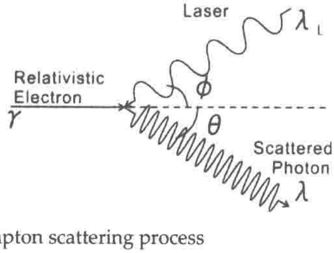

Figure 1. Schematic of laser-Compton scattering process

The major challenge of the laser Compton source for single shot imaging is the generation of threshold X-ray brightness, which in turn results in a clear sample imaging. Figure 1 describes the schematic of the laser-Compton interaction between electron beam and laser.

Laser-Compton scattering photon spectrum has a peak in the forward direction at a wavelength;

$$\lambda_p = \frac{\lambda_L(1+\frac{K^2}{2})}{2\gamma^2(1+\beta cos\phi)} \tag{1}$$

where γ and β are Lorentz factors, λ_L is the laser undulation period (laser wavelength), K is the K parameter of the undulator, which is equivalent to the laser intensity parameter, and Φ is the angle between electrons and laser propagation direction. The spectrum depends on the angular distribution; the wavelength λ is emitted at

$$\theta = \frac{1}{\gamma}\sqrt{\frac{\lambda-\lambda_p}{\lambda_p}} \tag{2}$$

It is seen that higher γ electron beam produces higher brightness of generated X-ray beams. The general formula of obtainable X-ray photon flux N_0 is calculated in the normal collision by the following expression,

$$N_0 \propto \frac{\sigma_c N_e N_p}{4\pi r^2} \tag{3}$$

where σ_c is the Compton cross section (6.7 x 10^{-25} cm^2), N_e is the total electron number, N_p is the total laser photon number, and r is the interaction area radius. Longer wavelength laser like ps CO_2 laser is advantageous to generate higher brightness X-rays at a fixed wavelength due to higher γ factor of employed electron beam, namely higher energy accelerator. Same energy laser pulse contains 10 times photons compared to solid state laser ones. Disadvantage is that the total system size becomes larger compared to the case of solid state laser based Compton source.

The approach to increase the photon flux is equivalent to increase N_e, N_p and decrease r, but there are instrumental limitations to realize these simultaneously. The practical limitation is the maximum electron number N_e and minimum interaction area diameter r. These are determined by emittance of the accelerated electron bunch and Coulomb repulsion. We would like to suppose it as 1nC, 3ps and focusable down to 10μm diameter at 38MeV acceleration energy. Another limitation is the onset of the nonlinear threshold of the higher harmonics generation, which is evident over 10^{17}W/cm^2 CO_2 laser irradiation intensity (Kumita, et.al. 2008). Laser pulses with 1ps pulse width focused down to 10μm, reaches at this threshold with 100mJ pulse energy. The nonlinear Compton threshold is characterized by the laser field strength

$$a_0 = eE/m\omega_L c \tag{4}$$

where E is the amplitude of laser electric field, ω_L is the laser frequency and c is the speed of light. The laser field strength is linearly depending on the laser wavelength. The laser energy for the nonlinear threshold of a_0~0.6 corresponds to 1J with 1ps at 10μm focusing in case of solid state laser. Single shot imaging was already realized by a 3J, 5ps CO_2 laser pulse focused onto 0.5nC, 32μm electron bunch (Oliva, et.al 2010). The focused laser intensity is over the nonlinear threshold as a_0>1. The X-ray spectrum was evidently overlapped with higher harmonics of X-rays. We can then estimate as it is also possible to expect a single shot imaging with equivalent solid state laser pulse, once it is possible to focus down to 10μm diameter to overcome the magnitude lower laser photon number. Table 1 summarizes the design laser parameters optimized for single shot imaging. It is clear from the table that a one pulse configuration is not possible to realize a single shot imaging because of the nonlinear threshold.

Nonlinear threshold	1J
Single shot imaging	4J
Pulse width	1ps
Focus diameter	10μm

Table 1. Solid state laser parameters for single shot imaging by Compton X-ray source

Usual approach is to increase the repetition rate of the event, and the obtainable X-ray photon average flux is expressed as;

$$N = f \times N_0 \tag{5}$$

where f is the repetition frequency. Fundamental characterization of the laser-Compton X-ray source has been undertaken with f typically as 1-10 Hz. High flux mode requires f in 100MHz range in burst mode for an equivalent single shot imaging.

The first approach is the pulsed laser storage in an optical enhancement cavity for laser-Compton X-ray sources (Sakaue, et.al. 2010, 2011). The enhancement factor P inside the optical cavity was 600 (circulating laser power was 42kW), in which the Finess was more than 2000, and the laser beam waist of 30μm (2σ) was stably achieved using a 1μm wavelength Nd:Vanadium mode-locked laser with repetition rate 357MHz, pulse width 7ps, and average power 7W. The schematic of the employed super-cavity is shown in Figure 2.

Short laser pulse *input* is injected through mirror 1 with transmittance T_1 and reflectance R_1. The mirror curvature is given as ρ. The beam waist is given as W_0 and the cavity length is given as L_{cav}. The injected pulses overlap with the following pulses inside the cavity indicated as *Stored*. The loss is caused due to transmissions T_1 and T_2 of both mirrors.

An enhancement cavity requires high reflectivity and low transmittance mirror i.e. ultra-low loss mirror as an input and high reflectivity mirror as an output for high enhancement. The enhancement P is expressed by using cavity finesse F as (Hodgson, et.al, 2005);

$$P = \frac{F}{\pi} \tag{6}$$

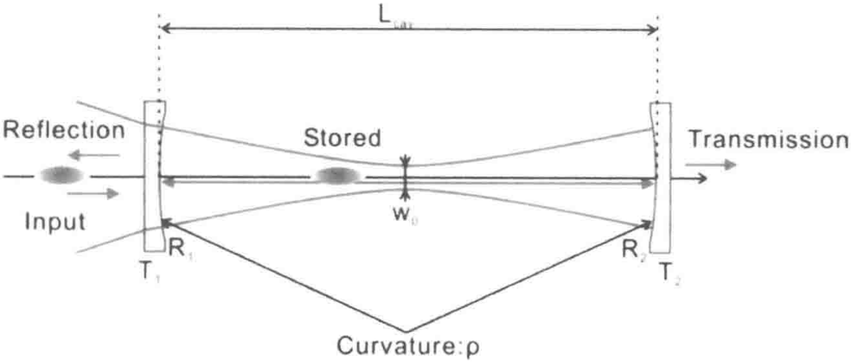

Figure 2. Schematic of laser storage enhancement cavity of Sakaue

It is noted that the assumed cavity length is perfectly matched with the repetition rate of input laser pulses. Finesse *F* is given by;

$$F = \frac{\pi\sqrt{R_{eff}}}{1 - R_{eff}} \tag{7}$$

where R_{eff} is $\sqrt{R_1R_2}$. As is described above, higher reflectivity provides a higher enhancement cavity. Particularly the loss, which includes both absorption and scattering on the reflection coating, is the critical issue for storing high power laser beam. The beam waist of an enhancement cavity is described as;

$$w_0^2 = \frac{\lambda}{\pi}\frac{\sqrt{L_{cav}(2\rho - L_{cav})}}{2} \tag{8}$$

where λ is the wavelength of the laser, L_{cav} is the cavity length, ϱ is the curvature of the cavity mirror. While high enhancement is relatively easier, smaller waist cavity down to 10μm is difficult as described in Eq. (8). Another work reported an enhancement of *P*~1400 with a 22 μm beam waist and 72kW storage power (Pupeza, et.al. 2010). The scaling limit is given by optics damage, which is around 100kW with ps pulse in this research stage. It was reported by Sakaue on an imaging demonstration by using the enhancement cavity approach of Fig.2, in which the stored pulse energy was 200μJ level in a burst mode of 100 pulses. The equivalent macro pulse energy was 20mJ. The larger focusing spot decreased available X-ray photons in each collision event, and the required time for imaging was much longer than equivalent single shot imaging (Sakaue, et.al, 2012). The repetition rate was 3Hz, and imaging of a fish bone was taken in 30 min with total laser energy of 108J. Figure 3 shows an imaging example in this experiment. Once the laser is focused to 10 μm diameter, and electron beam is focused to 30μm diameter, then the required total laser energy deceases to 3J, which indicates the design parameter of Table 1 as a good measure.

Grating based X-ray phase contrast imaging is now developing as a more sensitive imaging technology (Momose, et al. 2012), and a high repetition rate X-ray source, based on an enhancement cavity combined with a compact synchrotron, was recently introduced in preclinical demonstration of biological samples (M.Bech, et.al 2009). The X-ray peak energy was 13.5keV with 3% band width. The source size was relatively large as 165μm due to the focusing limit of circulating electron bunch in the compact ring. The repetition rate was typically in continuous 100MHz region, but the unit imaging time period was around 100 seconds (~2 minutes) due to lower X-ray photon flux per each event.

Classical low repetition rate laser Compton X-ray source demonstrated earlier a successful in-line phase contrast imaging of biological samples (Ikekura-Sekiguchi,et.al 2008). The repetition rate was at 10Hz with 40μm diameter source size. The imaging was undertaken by 3ps pulse width X-ray beam of 30keV energy. The required shot number for imaging was 18000 (30 minutes). It was indicated by this experiment that a solid state laser must have higher pulse energy more than 1J, and a better beam quality for 10μm focusing, for single shot imaging. We evaluate a possible solid state laser technology in the following sections on this subject, by reviewing practical instrumental limitations and propose the most promising approach for a compact single shot laser-Compton X-ray imaging.

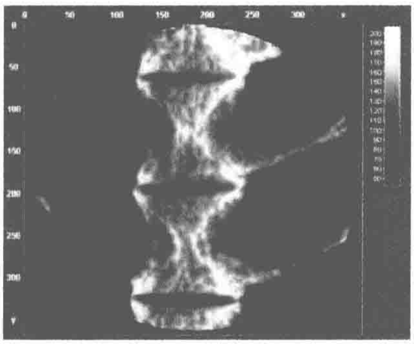

Figure 3. Refraction contrast imaging of bio sample (fish bone) by a laser-Compton X-ray source (Sakaue, et.al. 2012)

2. Temporal and spatial synchronization between electron beam and laser pulses

The essential technology for the laser-Compton X-ray source has been well studied in the Femtosecond Technology Project in Japan, and the achieved performance of the X-ray beam was also well characterized. Mathematical formula was obtained on its fluctuation depending on the temporal and spatial jitters (Yorozu, et.al 2002). Synchronization and stabilization technology was developed to the stage that the resulting pulse–pulse X-ray fluctuation almost reflects the laser pulse energy fluctuation (Yanagida, et.al 2003). The achieved overall performance was reported by T.Yanagida in a SPIE conference (Yanagida, et.al 2005). Figure 4 and table 2 show the system configuration and the summary of the specification of the laser-Compton X-ray source, studied and developed in the FESTA program. A phase contract imaging was also demonstrated by this light source of bubbles in solidified adhesives.

The electron beam is generated from a photo cathode RF gun driven by a synchronized picosecond UV laser, and accelerated to 38MeV energy by a S-band Linac. The achieved normalized emittance was 3 πmm-mrad, and resulted in the focused beam size as 30μm. It was demonstrated as further reduction of emittance was possible by spatial and temporal shaping of irradiation laser pulse for electron beam from photo cathode (Yang, et.al.2002). The employed laser for X-ray generation was a 4TW Ti:Sapphire laser with 800nm wavelength. The laser pulse was focused down to 10μm diameter and the peak intensity was around 10^{18} w/cm^2. The number of generated X-rays was measured with Micro Channel Plate located 2.6m downstream from the interaction point (source point). The MCP gain was calibrated using a standard ^{55}F X-ray source with known strength. The pulse width was estimated from measured electron beam and laser pulse width. The X-ray pulse width is almost determined by longer electron beam pulse width in case of normal incidence (165°interaction angle) and the cross section of the focused electron beam in case of 90°interaction angle. The long term fluctuation of the generated X-ray pulses is shown in Figure 5 in case of normal incidence arrangement. The repetition rate was 10Hz and the X-ray fluctuation was 6%, which is almost equivalent to the fluctuation of incident laser pulse energy. The laser focused intensity is around the nonlinear laser-Compton threshold as a_0~0.6. This was confirmed by a calculation by CAIN code in Figure 6. It is observed in the calculation of a nonlinear effect in the higher component of the generated X-ray energy distribution by blue dots (calculation by K.Sakaue).

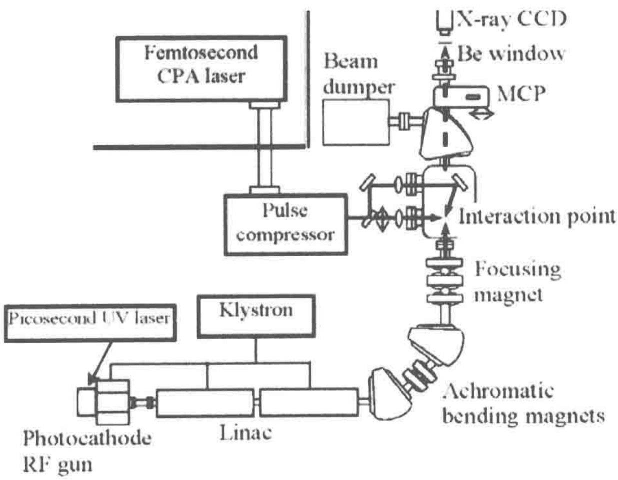

Figure 4. System configuration of laser-Compton X-ray source